J. Phys. Chem. A **2009,** *113,* 177–183

Theoretical Studies on Kinetics and Reactivity of the Gas-Phase Addition and H-Abstraction Reactions of Pyridine with Atomic Chlorine

Salma Parveen and Asit K. Chandra*

Department of Chemistry, North-Eastern Hill University, Shillong 793022, India

Received: June 18, 2008; Revised Manuscript Received: October 16, 2008

Theoretical investigations are carried out on the mechanism, kinetics, and thermochemistry for the reaction between pyridine and atomic chlorine with use of the hybrid density functional model BB1K, BHandHLYP, and the ab initio MP2 method. Both addition to and hydrogen abstraction reaction from all the potential sites are considered. Barrier heights and thermochemistry for all the possible addition and abstraction processes are calculated for the first time. This helps to identify the most reactive reaction channels in different temperature ranges. The DFT-based reactivity descriptors are used to elucidate the site selectivity for the addition and abstraction reactions. The results obtained from the BB1K method are found to be in reasonably good agreement with the available experimental results.

1. Introduction

The atmospheric chemistry of pyridine is important because of its presence in the atmosphere from industrial sources and also from coal combustion.[1,2] The reaction of pyridine with OH radical[3−5] and atomic chlorine[6] has drawn considerable attention in recent times because of its importance in atmospheric chemistry. Reaction with OH is generally assumed to be the major atmospheric degradation channel for pyridine. However, the importance of its reaction with atomic chlorine (Cl), especially in the coastal atmosphere, has also been emphasized.[6] In fact, several new investigations on coastal air have shown that photolysis of molecular chlorine can yield sufficiently high concentrations of Cl atoms to render the oxidation of common gaseous compounds by this species to compete or even be up to 100 times faster than the analogous reaction with the OH radical.[7−10] The rate constant for the reaction of halogenated aldehydes with Cl atoms is also known to be higher than the same for the similar oxidation reaction with OH radical.[11] The ion content of the troposphere influences the atmospheric electrical conductivity and ion recombination processes could trigger the formation of ultrafine aerosol particles.[12] This ion-induced nucleation process can have impact on earth's climate because of its potential role as cloud condensation nuclei.[13] The presence of the protonated ions of pyridine and its other derivatives has been detected by experimental measurement technique.[14]

There are many experimental[3,4] and theoretical[5] studies for the reaction of pyridine with OH radical. The OH-addition to the ring carbon atom is known to be the dominant reaction channel at lower temperature, whereas the hydrogen abstraction channel becomes important at higher temperature. It has also been shown that OH-addition is preferred at the meta site, on the other hand, ortho C−H bond is preferred for H-abstraction reaction. Similar site selectivity was also noticed for the reactions of pyridine with H and O (^{3}P).[5] However, there are very limited data for the reaction between pyridine and atomic chlorine (Cl), although this reaction is believed to be important for the atmospheric degradation of pyridine in coastal areas. In this work, we have studied in detail both addition reaction 1 and H-abstraction reaction 2 of pyridine with atomic chlorine using DFT and ab initio methods:

$$C_5H_5N + Cl \rightarrow C_5H_5N\text{-}Cl \qquad (1)$$

$$C_5H_5N + Cl \rightarrow C_5H_4N^{\bullet} + HCl \qquad (2)$$

Recently Wine and co-workers[6] have studied this reaction using laser flash photolysis-resonance fluorescence technique and noted that the formation of an adduct C_5H_5N-Cl is the major reaction channel at lower temperature. At higher temperature (>300 K), however, H-abstraction reaction becomes important and slowly predominates over the addition channel as temperature rises. It is difficult from experimental studies to identify the actual reaction center at which addition or abstraction may occur among the many potential sites for reaction. Theoretical studies can be very helpful to distinguish the actual reaction site and also to understand the reactivity and mechanism of the reaction. In this context, barrier heights for the Cl addition to all the potential sites and H-abstraction from the ortho, meta, and para C−H bonds of pyridine and the thermochemistry for all the possible addition and abstraction products (pyridinyl radical) are determined from the density functional theory (DFT) based BB1K,[15] BHandHLYP,[16] and ab initio Moller−Plesset perturbation theory up to second order (MP2)[17] calculations. Then the rate constants for these reaction channels are calculated to estimate the relative importance of these processes in the atmospheric degradation of pyridine.

It has been established both experimentally and theoretically that the Cl + pyridine system forms an adduct where Cl is bonded to the N atom of pyridine via a two-center-three-electron (2c-3e) bond.[18−20] The bond dissociation energy (BDE) of this N−Cl bond at 298 K was estimated to be 47.2 kJ/mol from the G2(MP2,SVP) calculation.[20] A similar value was also predicted from the experimental study and subsequent thermochemical analysis of the adduct formation.[6] Here apart from the Cl addition to the N-atom of pyridine, we have also studied the possibility of Cl addition to ring-carbon sites to understand the reactivity and thermochemistry for the other possible addition products. To our knowledge, this is the first detailed theoretical study for the Cl + pyridine system.

---

* Corresponding author. E-mail: akchandra@nehu.ac.in.

10.1021/jp805356z CCC: $40.75

Finally, DFT-based reactivity descriptors,[21] such as Fukui function (*f*) and local softness (*s*),[22] are used to understand the inherent reactivity of different sites of pyridine toward addition and abstraction reaction. These DFT-based reactivity descriptors are known to be efficient to elucidate the reactive behavior of a substrate.[23]

2. Computational Method

The geometries of pyridine, transition states (TS) for Cl addition and H-abstraction reactions, addition products, and pyridinyl radicals produced after hydrogen abstraction from pyridine were optimized by using the BB1K/6-31+G(d,p) method.[15] The BB1K method is specifically designed for kinetic calculations and is known to produce reliable thermodynamic and kinetic parameters for radical reactions including reactions with Cl atoms.[24,25] To check it further, we have studied the potential energy surface for the Cl atom−benzene complex and the results are compared with those reported by Hadad and coworkers.[26] Our BB1K results show that the π-complex (referred to as π-2c in ref 26) is the most stable complex, whereas the σ-complex (referred as σ-2c in ref 26) and the transition state ($TS_{\pi\text{-}\sigma}$) connecting the π- and σ-complex are 1.08 and 1.51 kcal mol^{-1}, respectively, higher in energy than the π-complex. These values agree quite well with the CASPT2 and PCM/BH&HLYP results reported in ref 26. The results obtained from BhandHLYP calculations are found to be similar to the BH&HLYP/6-311++G(d,p) results.[26] The detail results of benzene−Cl complexes are given as Supporting Information (Tables S1 and S2).

Frequency calculations were performed at each stationary point to characterize the minimum energy equilibrium structure and transition state. All these calculations were also performed by using the BHandHLYP/6-311G(d,p) method. The optimized structures obtained from BB1K and BHandHLYP were found to be quite close. But the barrier heights calculated from the results of BHandHLYP for addition and abstraction reactions were almost 2 kcal mol^{-1} higher than the BB1K results. Additionally, single-point ROMP2/6-311++G(d,p) calculations were performed at the BB1K optimized structure. Single configuration ab initio calculations may not be reliable for these systems because of high-spin contamination (the $\langle S^2 \rangle$ value was greater than 1.20 for doublet systems) for the open shell systems. In fact, UMP2 calculations could not be performed because of high spin contamination for the open shell systems and convergence problem. The $\langle S^2 \rangle$ values at the BB1K level for the open shell doublet addition TS and products remained in a range of 0.79−0.80, whereas for abstraction TS and pyridinyl radicals it was almost 0.76. The results obtained from the BB1K method are found to be more consistent with the experimental results and are presented here, whereas results obtained from the BhandHLYP and restricted open-shell MP2 (ROMP2) calculations are added as Supporting Information.

The equilibrium constant for adduct formation was calculated from the standard statistical mechanical formula[27]

$$K_p(T) = \frac{1}{k_B T} \frac{q_{C_5H_5N-Cl}(T)}{q_{C_5H_5N}(T) \cdot q_{Cl}(T)} \tag{3}$$

where q_x represents the partition function for the species x and k_B is the Boltzmann constant. The translational partition function was evaluated per unit volume. The ground $^2P_{3/2}$ and excited $^2P_{1/2}$ electronic states of Cl atom, with a splitting of 881 cm^{-1} due to spin−orbit coupling, were used for the calculation of the electronic partition function. Proper symmetry number (2) was also used while calculating the rotational partition functions for pyridine, C_5H_5N-Cl adduct, and 4-pyridinyl radical.

The H-abstraction rate constant was estimated by using the conventional transition state theory (TST):[28]

$$k(T) = \Gamma(T) \frac{k_B T}{h} \frac{q_{TS}(T)}{q_{C_5H_5N}(T) \cdot q_{Cl}(T)} e^{-\Delta E_0^{\#}/RT} \tag{4}$$

where $\Gamma(T)$ is the transmission coefficient and $\Delta E_0^{\#}$ is the barrier height. The transmission coefficient $\Gamma(T)$ was calculated from Wigner's formula.[29] At higher temperature (>300 K), $\Gamma(T)$ was found to be almost unity. All electronic structure calculations were performed with the Gaussian-03 program.[30]

3. Results and Discussion:

The reaction of pyridine with Cl can be divided into two major processes, namely addition of Cl to pyridine and abstraction of H from pyridine. The results for each of these channels are presented and discussed separately.

A. Addition Reaction. As mentioned before, previous experimental study[6] predicted the addition of Cl to the N-atom of pyridine as the dominant reaction channel at lower temperature ($T < 270$ K). The formation of such adduct and the nature of the N−Cl bond were also studied by using quantum chemical methods.[18−20] The BB1K optimized structure of this adduct (C_5H_5N-Cl) is shown in Figure 1 and the optimized geometrical parameters are given in Table 1. Our calculated N−Cl bond length of 2.36 Å is found to be close to the value of 2.39 Å obtained from the UMP2(full)/6-31G(d) optimization. Although the loose bond formation between N and Cl atoms in this adduct does not have much effect on the other structural parameters of pyridine, it is interesting to note the shortening of the C−H bond in the C_5H_5N-Cl adduct (given in Table S3 of the Supporting Information), especially at the ortho position. The C−H bond length at the ortho position (1.0819 Å) is seen to be longer by 0.002 Å from the other C−H bonds in pyridine, but all the C−H bond lengths become almost equal in the adduct due to greater shortening of the ortho C−H bond (by 0.002 Å). It has been observed from NBO analysis[31] that the σ^*(C−H) population for the ortho C−H bond (0.0204 e) is larger than the other C−H bonds (0.0127 e) in free pyridine. In C_5H_5N-Cl adduct, the Cl atom partially ties up the nitrogen lone pair and reduces the σ^*(C−H) population for the ortho C−H to a much greater extent than the other C−H bonds, resulting in a significant decrease in this bond length. The signature of this bond shortening for the ortho C−H bond can also be seen from the blue shift of the C−H stretching frequency while going from pyridine to the C_5H_5N-Cl adduct. A blue shift of 34 cm^{-1} is observed for the ortho C−H bond, whereas the same for other C−H bonds amouts to 7−10 cm^{-1} only. The N−Cl stretching frequency in C_5H_5N-Cl is calculated to be 198 cm^{-1} and the force constant of the N−Cl bond is 0.337 mdyne/Å, signifying the formation of a weak N−Cl bond. Vibrational frequencies and rotational constants obtained from the BB1K calculations are given in Table S4 of the Supporting Information, whereas the results of BhandHLYP and ROMP2 calculations are listed in Tables S5−S7 in the Supporting Information.

The transition state for the addition to the N-atom site of pyridine could not be located. The energy shows only an asymptotic behavior while increasing the N−Cl bond length from its equilibrium value and thus this addition process is likely to be barrierless. The results of our calculation are listed in Table 2. The calculated free energy change ($\Delta_r G_{298}$) value of −5.5 kcal mol^{-1} (experimental value is −4.3 kcal mol^{-1}) indicates

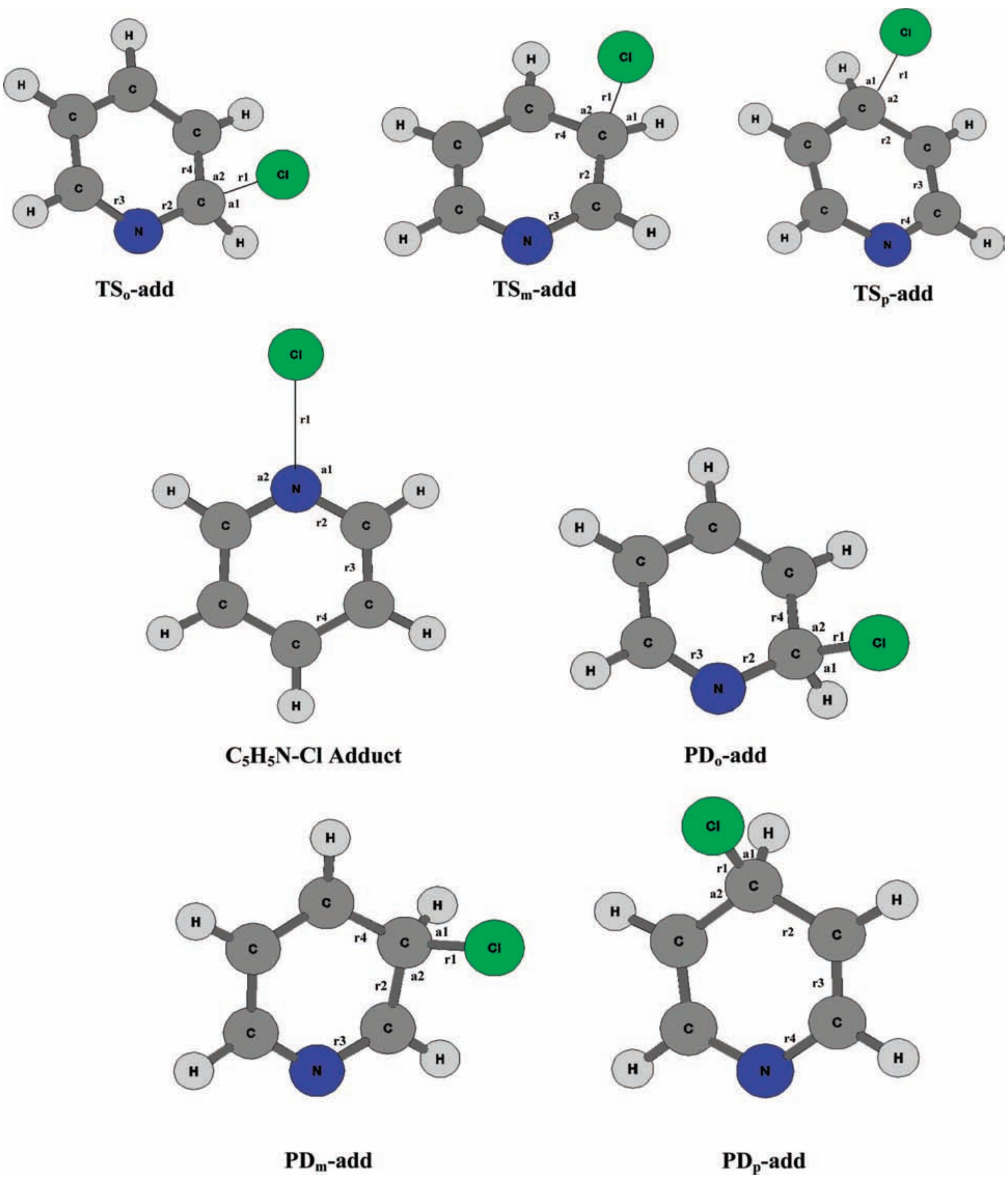

TS_o-add TS_m-add TS_p-add

C_5H_5N-Cl Adduct PD_o-add

PD_m-add PD_p-add

Figure 1. The structures of transition states (TS_x-add) for Cl addition to ortho, meta, and para carbon atoms of pyridine, the corresponding addition products (PD_x-add), and C_5H_5N-Cl adduct.

that addition of Cl to the N-atom of pyridine should be a spontaneous process at this temperature.

In addition to the Cl atom addition to the N-atom of pyridine, the possibility of Cl addition to ring-carbon atoms is also considered. The optimized TS structures and addition products for Cl addition to ring carbons are presented in Figure 1 and the geometrical parameters are listed in Table 1. The energy, enthalpy, and free energy barrier for the addition of Cl to the ring-carbon sites and reaction enthalpy and free energies for these reactions are thus calculated. These results are given in Table 2. The barrier height for addition to all the ring-carbon atoms is found to be negative and the meta carbon site is found to be most reactive. A similar observation was made for H, O, and OH addition to pyridine as well.[5] The enthalpy change ($\Delta_r H$) values for the addition of Cl to ortho, meta, and para ring-carbon at 298 K are −4.8, −6.2, and −3.8 kcal mol^{-1}. Thus energetically, addition of Cl to the N-atom site is preferred over that to the ring-carbon sites. Moreover, although $\Delta_r H$ values for addition to the carbon site are seen to be negative (exoergic reaction), free energy change ($\Delta_r G$) for this reaction becomes positive in the temperature range (200−450 K) studied here, because of the large negative entropy factor. Hence addition of Cl to ring-carbons is not a favorable process unless the temperature is very low. Moreover, at thermal equilibrium,

TABLE 1: The BB1K Optimized Geometrical Parameters (as shown in Figures 1 and 2) for the Transition states (TS_x-add) and Products (PD_x-add) of Cl-Addition to Ring-Carbons, the C_5H_5N-Cl Adduct, and the Transition States (TS_x-abs) of H-Abstraction from the Ortho, Meta, and Para C−H Bonds of Pyridine[a]

system	r_1	r_2	r_3	r_4	a_1	a_2
Cl-addition						
TS_o-add	2.150	1.368	1.302	1.409	91.8	98.4
TS_m-add	2.118	1.437	1.307	1.428	92.8	104.7
TS_p-add	2.129	1.428	1.372	1.336	91.9	102.8
$C_5H_5N{-}Cl$	2.358	1.319	1.384	1.385	119.4	119.4
PD_o-add	1.855	1.416	1.291	1.473	101.2	106.8
PD_m-add	1.880	1.476	1.296	1.357	100.4	107.4
PD_p-add	1.856	1.468	1.361	1.346	101.1	108.9
H-abstraction						
TS_o-abs	1.574	1.375	1.382	1.269	174.0	117.5
TS_m-abs	1.720	1.332	1.366	1.371	178.6	116.8
TS_p-abs	1.650	1.346	1.364	1.396	180.0	117.5

[a] Bond lengths (r) and angles (a) are given in Å and deg, respectively.

Boltzmann distribution suggests that N-addition product will be the primary addition product and population of chloropyridienyl radicals will be negligible because of the much lower energy of the former adduct. On the other hand, Δ_rG_{298} values for H, O, and OH addition to ring-carbons of pyridine were found to be negative even at 298 K because of higher exothermicity of these reactions.[5] The Δ_rG values also suggest that addition of Cl to the N-atom of pyridine should be the only important addition channel for the reaction of Cl and pyridine. On the contrary, Turecek et al.[32] observed that addition of the OH radical to the N-atom of pyridine generating the C_5H_5N-OH radical was unlikely to occur because of a large energy barrier (11.7 kcal mol^{-1}) to this process and addition of OH to ring-carbon sites (mainly at the meta position) was found to be the main addition channel. Therefore, the mechanism for OH and Cl addition to pyridine appears to be different. At higher temperature (>300 K), the negative entropy factor slowly overwhelms the exothermicity of this addition reaction and makes it unfeasible to occur.

The equilibrium constant (K_p) values for the C_5H_5N-Cl adduct formation are calculated in the temperature range of 216−270 K by using eq 3 to compare with the experimental result. The following equation is then derived from a van't Hoff plot of these data:

$$\ln K_p = -12.05 + 6341/T \qquad (5)$$

This equation compares reasonably well with that derived from the experimental data: $\ln K_p = (-11.87 \pm 0.96) + (5700 \pm 130)/T$. The change in enthalpy (Δ_rH_{298}) and entropy (Δ_rS_{298}) estimated from the slope and intercept of the van't Hoff plot are −12.6 kcal mol^{-1} and −23.9 cal mol^{-1} K^{-1}, respectively. Our calculated Δ_rH_{298} value is somewhat lower than the experimental value of −11.3 ± 0.7 kcal mol^{-1} and as a result our calculated K_p value (1.7×10^6 atm^{-1}) is found to be higher than the experimental value (1.35×10^5 atm^{-1}) at 240 K.[6] The calculated Δ_rS_{298} value is in good agreement with the experimental value of −23.6 ± 1.5 cal mol^{-1} K^{-1}.[6] The K_p values for different temperatures within 216−270 K are listed in Table S8 of the Supporting Information.

As the adduct (C_5H_5N-Cl) formation is found to be a barrierless process, the formation of the adduct at lower temperature is expected to be related to the collision frequency of Cl and pyridine. We have calculated the collision frequency factor using the standard formula.[28] The value of d_{AB} (mean of molecular diameters) is obtained from the estimated radius of pyridine (2.93 Å)[33] and covalent radius of Cl (0.99 Å).[34] The rate constant (k_{add}) value estimated from this simple and qualitative approach is 2.46×10^{-10} cm^3 molecule^{-1} s^{-1} at 298 K. The value obtained from this approach is almost an order of magnitude higher than the experimentally predicted value of 5×10^{-11} cm^3 molecule^{-1} s^{-1}. This is mainly because of the assumption that each collision leads to the adduct formation, neglecting the orientation factor. A steric factor [$p = k_{add}(\text{exptl})/k_{add}(\text{calcd})$] of 0.2 brings the collision theory based rate constant almost equal to the experimentally predicted value. This value of the steric factor (0.2) seems reasonable from the fact that there is only one N-site out of six possible sites of attack in pyridine ring and also it is known that the steric factor for the gas-phase atom−molecule reaction is generally of the order of 0.1. Of course, this simple approach is unlikely to give the correct temperature variation of k_{add}. But at higher temperature, however, decomposition of C_5H_5N-Cl to pyridine and Cl will be faster and the lifetime for this adduct is likely to be very small. The rapid decrease of K_p with increasing temperature shows that unimolecular dissociation of the C_5H_5N-Cl adduct becomes very fast and the adduct immediately dissociates to pyridine and Cl.

B. Hydrogen Abstraction Reaction. The TS structures for the H-abstraction from C−H bonds at the ortho, meta, and para positions and the structures of the resulting pyridinyl radicals are determined by using the BB1K method. These TS structures are presented in Figure 2. The breaking C−H bond length increases by almost 0.5 Å in TS compared to the value in pyridine, whereas the forming H−Cl bond is found to be longer by only 0.1 Å from the bond length in free HCl. This signifies the formation of a late TS, which is of course expected from Hammond's principle for endothermic reaction. The results of our calculations are summarized in Table 2. It is clear from the barrier height values in Table 2 that for the H-abstraction reaction, the ortho C−H bond, having the lowest barrier height, is the most reactive site, whereas abstraction from the meta position is most difficult. Similar reactivity behavior was also observed for the H-abstraction reaction of pyridine with H, O, and OH radical.[5] But the H-abstraction barrier height for Cl is substantially larger than that observed for H, O, and OH radical. In fact, the C−H bond at the ortho position is weaker than the other two C−H bonds of pyridine. The BB1K (BhandHLYP) calculated bond dissociation enthalpy (BDE) at 298 K for the ortho C−H bond is 104.8 (104.4) kcal mol^{-1}, whereas those for meta and para C−H bonds are 111.1 (110.5) and 109.3 (108.8) kcal mol^{-1}, respectively. The exact H-atom energy (–0.5 a.u.) is used for BDE calculations. The BDE values calculated from the ROMP2 method for the ortho, meta, and para C−H bonds are 104.2, 109.9, and 108.6 kcal mol^{-1}, respectively. The BDE values estimated from the BB1K and BhandHLYP methods are found to be quite close to the values reported for ortho (104.7 kcal mol^{-1}), meta (110.9 kcal mol^{-1}), and para (109.5 kcal mol^{-1}) C−H bonds of pyridine from the B3LYP/6-311+G(2d,p) calculations[6] and also to the BDE values obtained from the pyrolysis experiment for ortho (105.0 kcal mol^{-1}), meta (112.0 kcal mol^{-1}), and para (112.0 kcal mol^{-1}) C−H bonds of pyridine.[35] This difference in BDE values for the three C−H bonds is also reflected in the C−H bond length, as discussed earlier. Thus H-abstraction from the ortho C−H bond should be easier, since BDE of the C−H bond is known to be well correlated with the reactivity toward the H-abstraction reaction.[36]

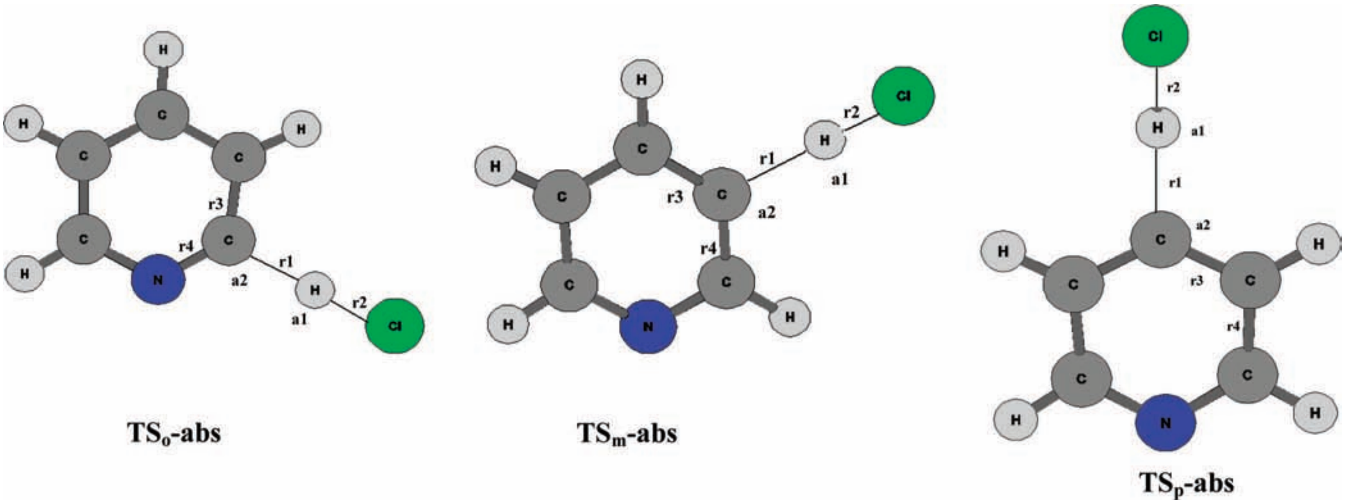

TS_o-abs TS_m-abs TS_p-abs

Figure 2. The structures of transition states (TS_x-abs) for H-abstraction by Cl from ortho, meta, and para C−H bonds of pyridine.

TABLE 2: Energy ($\Delta E^{\#}$), Enthalpy ($\Delta H^{\#}$), and Free Energy ($\Delta G^{\#}$) Barrier Height and Reaction Enthalpy (Δ_rH) and Free energy (Δ_rG) for Cl-Addition to Pyridine and H-Abstraction from Pyridine by Cl Atom As Obtained from the BB1K Method at 298 K[b]

TS		$\Delta E^{\#}$	$\Delta H^{\#}$	$\Delta G^{\#}$	Δ_rH	Δ_rG
adduct (C_5H_5N-Cl)					−12.55 (−11.28)[a]	−5.46 (−4.29)[a]
Cl-addition to ring carbon	ortho	−2.57	−3.14	4.95	−4.80	3.05
	meta	−5.00	−5.53	2.47	−6.16	1.57
	para	−1.84	−2.39	5.64	−3.76	4.12
H-abstraction by Cl	ortho	3.07	2.73	9.67	6.73	2.90
	meta	10.55	10.25	17.22	12.94	9.12
	para	8.79	8.54	15.07	11.21	7.80

[a] Experimental value from ref 6. [b] Data are in kcal mol^{-1}.

As shown in Table 2, the Δ_rH and Δ_rG values for the H-abstraction reactions are positive even at 298 K. Barrier heights are also positive for abstraction reactions. Thus at lower temperature (<298 K), only the addition process is likely to be the main reaction channel between Cl and pyridine. A similar conclusion was made from the experimental study as well. The temperature variation of the Δ_rG value for the addition of Cl to N-atom and the meta carbon site of pyridine and H-abstraction from the ortho C−H bond is shown in Figure 3. As temperature increases the Δ_rG value for the abstraction channel slowly becomes negative and that for the addition channel goes to positive. Thus at higher temperature H-abstraction will be the major process for the reaction between Cl and pyridine.

The total rate constant values for H-abstraction reactions between pyridine and Cl as calculated from the TST eq 4 are listed in Table 3. Although there are three potential H-abstraction sites in pyridine, effectively H-abstraction from the ortho C−H bond is the only channel to contribute. The rate constant values for H-abstraction from meta and para positions are found to be 2-order of magnitude lower than that for the ortho position. The TST calculated high-pressure limit rate constant value for the abstraction process amounts to 4.46×10^{-14} cm^3 $molecule^{-1}$ s^{-1} at 300 K. As is evident from the ratio $k_{abs}(\text{exptl})/k_{abs}(\text{calcd})$ given in Table 3, the calculated value is somewhat lower than the experimental value.

The rate constant values for H-abstraction over the temperature range 299−435 K are plotted in Arrhenius form in Figure 4. The Arrhenius expression for kinetic data obtained over this temperature range (299−435 K) is

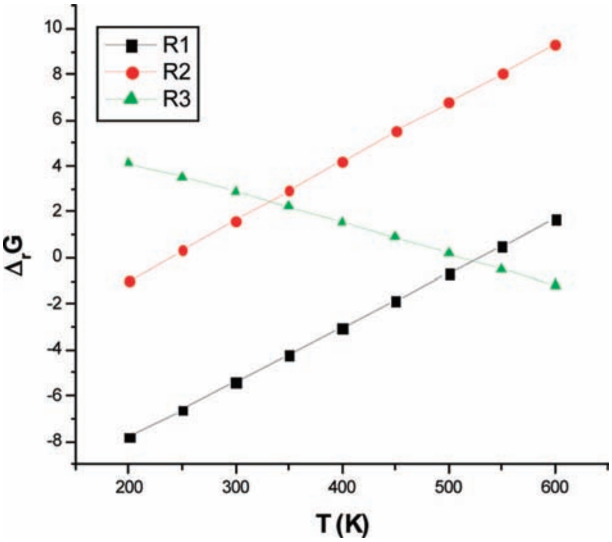

Figure 3. Variation of free energy change (Δ_rG in kcal mol^{-1}) with temperature for Cl addition to N-atom (R1), meta carbon atom (R2), and H-abstraction by Cl from ortho C−H bond (R3) of pyridine.

$$k_{abs}(T) = 4.51 \times 10^{-11} \exp(-2073/T) \text{ cm}^3 \text{ molecule}^{-1} \text{ s}^{-1} \tag{6}$$

The Arrhenius expression obtained from the experimental data over the same temperature range is $k_{abs}(T) = (2.08 \pm 0.47) \times 10^{-11} \exp(-(1410 \pm 80)/T)$ cm^3 $molecule^{-1}$ s^{-1}. Our calculated pre-exponential factor compares well with the experimental value, but the computed activation energy (4.1 kcal mol^{-1}) is somewhat higher than the experimental value of 2.8 ± 0.2 kcal

TABLE 3: The Calculated and Experimental Rate Constants (k_{abs} in cm^3 molecule^{-1} s^{-1}) for H-Abstraction Reactions of Pyridine and Cl Atom

	$k_{abs} \times 10^{13}$		
T (K)	calcd	exptl[a]	k(exptl)/k(calcd)
299	0.45	1.44	3.2
320	0.69	2.10	3.0
335	0.91	2.67	2.9
340	1.00		
354	1.27	3.31	2.6
387	2.10	5.22	2.5
413	2.98	6.33	2.1
435	3.91	8.10	2.1

[a] Reference 6.

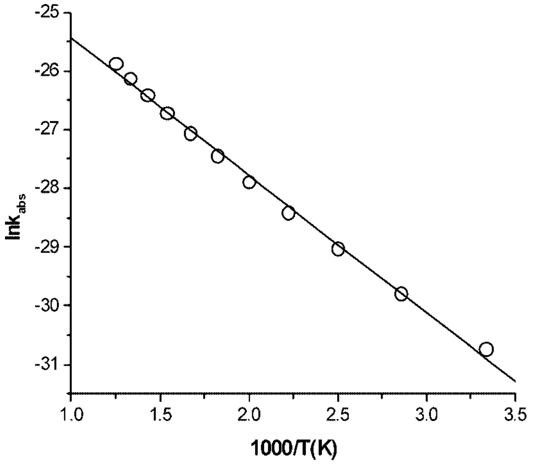

Figure 4. The Arrhenius plot of H-abstraction rate constant (k_{abs}) and temperature (T) for H-abstraction reaction between Cl and pyridine.

mol^{-1}. As a result calculated rate constant values for H-abstraction are found to be slightly lower than the experimental value. The calculated and experimental k_{abs} values become almost the same if the activation energy is scaled to 3.5 kcal mol^{-1}. The Arrhenius equation obtained from the fitting of kinetic data within a wider temperature range 300−800 K is

$$k_{abs}(T) = 9.37 \times 10^{-11} \exp(-2344/T) \text{ cm}^3 \text{ molecule}^{-1} \text{ s}^{-1} \quad (7)$$

The total rate constant (k_{tot}) at any given temperature should be the sum of rate constants for addition (k_{add}) and H-abstraction (k_{abs}) reactions. Since addition reaction dominates at lower temperature (<298 K) and k_{add} is almost 2 orders of magnitude greater than k_{abs} the total rate constant should be of the order of 10^{-11} cm^3 molecule^{-1} s^{-1}. At higher temperature (especially over 350 K), k_{tot} should be close to k_{abs}, because rapid dissociation of adducts to pyridine and Cl and hence loss of pyridine will be primarily due to abstraction reactions. Thus k_{tot} should then follow the similar Arrhenius equation obtained for k_{abs} (eq 7) at higher temperature.

The standard heats of formation values ($\Delta_f H^0_{298}$) at 298 K are estimated from the calculated heats of reaction ($\Delta_r H$) and the experimental heats of formation values for pyridine (33.5 kcal mol^{-1}), chlorine (29.0 kcal mol^{-1}), and HCl (−22.1 kcal mol^{-1}).[37] The calculated $\Delta_f H_{298}$ values are listed in Table 4. The calculated $\Delta_f H_{298}$ for C_5H_5N-Cl is 49.9 kcal mol^{-1}, which is close to the value (51.7 kcal mol^{-1}) estimated from experimental data.[6]

TABLE 4: The Values of Standard Enthalpy of Formation ($\Delta_f H^0_{298}$) of C_5H_5N-Cl, Product of Cl Addition to Ring-Carbons [chlorohydropyridine (Cl-PYD) radical], and Pyridinyl Radicals Produced after H-Abstraction from Pyridine

system	$\Delta_f H^0_{298}$ (kcal mol^{-1})
C_5H_5N-Cl	49.95
2-Cl-PYD	57.72
3-Cl-PYD	56.34
4-Cl-PYD	58.74
2-pyridinyl radical	91.29
3-pyridinyl radical	97.51
4-pyridinyl radical	95.73

4. Reactivity of Pyridine

The barrier heights and heats of reactions for the addition and H-abstraction reaction of Cl with pyridine show a definite trend of reactivity and site-selectivity. It has been observed from our theoretical results, as well as from experiment, that the N-atom is the preferred site for Cl addition and the meta position is the most preferable among the ring-carbon sites. Meanwhile the ortho position is found to be the most reactive site for the H-abstraction reaction. We thought that it would be interesting to see whether a similar reactivity trend can be obtained from the DFT-based reactivity parameters. These reactivity parameters have been found to be successful in many radical addition and H-abstraction reactions.[23,38] It has also been shown recently that local softness is well suited to predict the preferred hydrogen for abstraction from a substrate.[39] We have calculated softness (S), condensed to atom Fukui function (f_k^0),[40] and local softness (s_k^0) values for radical attack for all the atoms in pyridine using the standard working formula

$$S = 1/(\mathrm{IE} - \mathrm{EA})$$

$$f_k^0 = \frac{1}{2}[q_k(N+1) - q_k(N-1)]$$

$$s_k^0 = S f_k^0$$

where IE and EA are the vertical ionization energy and electron affinity, respectively, for a N-electron system, and $q_k(N+1)$ and $q_k(N-1)$ are electronic population on atom k for the $N+1$ and $N-1$ electronic systems. The B3LYP/6-311G(d,p) method[41] and CHELPG scheme, which is based on electrostatic potential driven atomic charges, were used for calculating these reactivity parameters. This scheme is known to provide reliable reactivity parameters.[39]

The results of our calculations of these reactivity parameters are listed in Table 5. The f_k^0 or s_k^0 values for the N-atom are found to be higher than that for ring-carbon atoms. Among the ring-carbon atoms, meta carbon has the highest s_k^0 value. Thus the N-atom of pyridine should be the most preferred site for Cl addition, whereas among ring-carbon sites Cl-addition to the meta carbon site should be preferable. Interestingly, a similar reactivity pattern has been observed from our calculated barrier height and reaction energy.

The s_k^0 values for the ortho (H7), meta (H8), and para (H9) hydrogens are seen to be in order H7 > H9 > H8. These s_k^0 values suggest that the ortho hydrogen should be the most preferred one for abstraction and the meta hydrogen will be the least preferred for abstraction. As a matter of fact, similar observations have indeed been made from our calculations for

TABLE 5: Global Softness (S in au^{-1}), Condensed to Atom Fukui Function (f_k^0), and Softness (s_k^0) Calculated from B3LYP/6-311G(d,p) Results

	S	atom	f_k^0	s_k^0
C_5H_5N	2.515	N1	0.4715	1.1859
		C2	−0.1672	−0.4205
		C3	0.1891	0.4756
		C4	0.0037	0.0092
		H7	0.1343	0.3376
		H8	0.0554	0.1394
		H9	0.1003	0.2524
Cl	2.876			

H-abstraction reactions of pyridine with Cl and also by others for different radicals.[5]

5. Summary and Conclusions

Theoretical studies on the reaction between Cl and pyridine have been carried out by using the hybrid DFT method BB1K. It has been observed that the addition of Cl to the pyridine N-atom forming an adduct (C_5H_5N-Cl) through a weak N−Cl bond is the primary reaction channel at lower temperature. The BDE of the N−Cl bond in C_5H_5N-Cl is estimated to be −12.5 kcal mol^{-1}. The calculated equilibrium constant (K_p) value for C_5H_5N-Cl adduct formation is 1.7×10^6 atm^{-1} at 240 K. The van't Hoff equation obtained from the temperature variation of K_p in the range 216−270 K is the following: $\ln K_p = -12.05 + 6341/T$.

The barrier heights for addition to ring-carbon sites are found to be negative, but Δ_rG values are positive even at 200 K and thus these processes are unlikely to contribute in the addition reaction. The ortho hydrogen is seen to be the most preferred for abstraction. At higher temperature, the Δ_rG value for H-abstraction from the ortho C−H bond becomes negative and the abstraction process is likely to be the main reaction channel. The Δ_rG value for the C_5H_5N-Cl adduct formation becomes positive at higher temperature and thus it is unlikely to exist because of a faster rate of dissociation of C_5H_5N-Cl to pyridine and Cl. The Arrhenius equation obtained from the fitting of kinetic data for the H-abstraction reaction over a temperature range of 300 − 800 K is the following: $k_{abs}(T) = 9.37 \times 10^{-11} \exp(-2344/T)$ cm^3 molecule^{-1} s^{-1}.

The k_{tot} should have a similar temperature dependence as $k_{abs}(T)$ within this temperature range as H-abstraction will be the main reaction for the loss of pyridine at this temperature range. The DFT-based local reactivity descriptor, s_k^0, correctly describes the observed reactive behavior of pyridine toward addition and abstraction reactions. The N-atom with the highest s_k^0 value is the most reactive site for Cl addition, whereas the H-atom at the ortho C−H bond has the highest s_k^0 value among the three hydrogens and was found to be the most preferred one for abstraction.

Acknowledgment. A.K.C. thanks DST, India for financial support through Project No. SR/S1/PC-13/2005 and UGC, India for providing computational facility under a special assistance program (SAP). Thanks are also due to the Reviewers for their constructive comments to improve the paper.

Supporting Information Available: The optimized structures and vibrational frequencies of all the species involved in the present study, and the barrier heights, heats of reaction, and free energy change for addition and abstraction reaction of pyridine with Cl. This material is available free of charge via the Internet at http://pubs.acs.org.

References and Notes

(1) Clemo, G. R. *Tetrahedron* **1973**, *29*, 3987.
(2) ATSDR toxicological profile, parts 4 and 5: http://www.atsdr.cdc.gov/toxoprofiles.
(3) Atkinson, R.; Tuazon, E. C.; Wallington, T. J.; Aschmann, S. M.; Arey, J.; Winer, A. M.; Pitts, J. N., Jr. *Environ. Sci. Technol.* **1987**, *21*, 64.
(4) Yeung, L. Y.; Elrod, M. J. *J. Phys. Chem. A* **2003**, *107*, 4470.
(5) Barckholtz, C.; Barckholtz, T. A.; Hadad, C. M. *J. Phys. Chem. A* **2001**, *105*, 140.
(6) Zhao, Z.; Huskey, D. T.; Olsen, K. J.; Nicovich, J. M.; McKee, M. L.; Wine, P. H. *Phys. Chem. Chem. Phys.* **2007**, *9*, 4383.
(7) Singh, H. B.; Kasting, J. F. *J. Atmos. Chem.* **1988**, *7*, 261.
(8) Finlayson-Pitts, B. J. *Res. Chem. Intermed.* **1993**, *19*, 235.
(9) Spicer, C. W.; Chapman, E. G.; Finlayson-Pitts, B. J.; Plastridge, R. A.; Hubbe, J. M.; Fast, J. D.; Berkowitz, C. M. *Nature* **1998**, *394*, 353.
(10) Oum, K. W.; Lakin, M. J.; DeHaan, D. O.; Brauers, T.; Finlayson-Pitts, B. J. *Science* **1998**, *279*, 74.
(11) Wang, Y.; Liu, J.-Y.; Li, Z.-S.; Wang, L.; Wu, J.-Y.; Sun, C.-C. *Chem. Phys.* **2006**, *324*, 609.
(12) Yu, F.; Turco, R. P. *Geophys. Res. Lett.* **2000**, *27*, 883.
(13) Charlson, R. J.; Lovelock, J. E.; Andreae, M. O.; Warren, S. G. *Nature* **1987**, *326*, 655.
(14) Eisele, F. L. *J. Geophys. Res.* **1988**, *93*, 716.
(15) Zhao, Y.; Lynch, B. J.; Truhlar, D. G. *J. Phys. Chem. A* **2004**, *108*, 2715.
(16) Becke, A. D. *J. Chem. Phys.* **1993**, *98*, 5648.
(17) (a) Moller, C.; Plesset, M. S. *Phys. Rev.* **1934**, *46*, 618. (b) Head-Gordon, M.; Pople, J. A.; Frisch, M. J. *Chem. Phys. Lett.* **1988**, *153*, 503. (c) Frisch, M. J.; Head-Gordon, M.; Pople, J. A. *Chem. Phys. Lett.* **1990**, *166*, 275. (d) Saebo, S.; Almlof, S. *Chem. Phys. Lett.* **1989**, *154*, 83.
(18) Breslow, R.; Brandl, M.; Hunger, J.; Turro, N.; Cassidy, K.; Krogh-Jespersen, K.; Westbrook, J. D. *J. Am. Chem. Soc.* **1987**, *109*, 7204.
(19) Abu-Raqabah, A.; Symons, M. C. R. *J. Am. Chem. Soc.* **1990**, *112*, 8614.
(20) McKee, M. L.; Nicolaides, A.; Radom, L. *J. Am. Chem. Soc.* **1996**, *118*, 10571.
(21) Parr, R. G.; Yang, W. *Density Functional Theory of Atoms and Molecules*; Oxford University Press: New York, 1989.
(22) (a) Parr, R. G.; Yang, W. *J. Am. Chem. Soc.* **1984**, *106*, 4049. (b) Yang, W.; Parr, R. G. *Proc. Natl. Acad. Sci. U.S.A.* **1985**, *82*, 6723.
(23) Geerlings, P.; Proft, F. de.; Langenaeker, W. *Chem. Rev.* **2003**, *103*, 1793. Chandra, A. K.; Nguyen, M. T. *Faraday Discuss.* **2007**, *135*, 191.
(24) Tiu, G. C.; Tao, F. *Chem. Phys. Lett.* **2006**, *428*, 42.
(25) (a) Gao, H.; Wang, Y.; Liu, J.; Yang, L.; Li, Z.; Sun, C. *J. Phys. Chem. A* **2008**, *112*, 4176. (b) Hemelsoet, K.; Moran, D.; Speybroeck, V. V.; Waroquier, M.; Radom, L. *J. Phys. Chem. A* **2006**, *110*, 8942.
(26) Tsao, M.-L.; Hadad, C. M.; Platz, M. S. *J. Am. Chem. Soc.* **2003**, *125*, 8390.
(27) McQuarrie, D. A. *Statistical Mechanics*, 1st Indian ed., VIVA Books: New Delhi, India, 2003.
(28) Laidler, K. J. *Chemical Kinetics*, 3rd ed.; Pearson Education: Delhi, India, 2004.
(29) Wigner, E. P. *Z. Phys. Chem.* **1932**, *B19*, 203.
(30) Frisch, M. J. et al . *Gaussian 03*, Revision C.01; Gaussian Inc.: Wallingford, CT, 2004.
(31) Reed, A. E.; Curtiss, L. A.; Weinhold, F. *Chem. Rev.* **1988**, *88*, 899.
(32) Vivekananda, S.; Wolken, J. K.; Turecek, F. *J. Phys. Chem. A* **2001**, *105*, 9141.
(33) The radius of pyridine was estimated by calculating its volume using the "Volume" option in the Gaussian-03 program.
(34) Cotton, F. A.; Wilkinson, G.; Murillo, C. A.; Bochmann, M. *Advanced Inorganic Chemistry*, 6th ed.; John Wiley & Sons: New York, 1999; p 548.
(35) Kiefer, J. H.; Zhang, Q.; Kern, R. D.; Yao, J.; Jursic, B. *J. Phys. Chem. A* **1997**, *101*, 7061.
(36) (a) Chandra, A. K.; Uchimaru, T. *J. Phys. Chem. A* **2000**, *104*, 9244. (b) Chandra, A. K.; Uchimaru, T. *Chem. Phys. Lett.* **2001**, *334*, 200.
(37) NIST Chemistry Webbook, Number 69, June, 2005: http://webbook.nist.gov/chemistry/.
(38) Nguyen, H. M. T.; Peeters, J.; Nguyen, M. T.; Chandra, A. K. *J. Phys. Chem. A* **2004**, *108*, 484.
(39) Hemelsoet, K.; van Speybroeck, V.; Waroquier, M. *Chem. Phys. Lett.* **2007**, *444*, 17.
(40) Yang, W.; Mortier, W. J. *J. Am. Chem. Soc.* **1986**, *108*, 5708.
(41) Lee, C.; Yang, W.; Parr, R. G. *Phys. Rev. B* **1988**, *37B*, 785.

JP805356Z